

Growing Momentum in the Various Field of Robotics- A Review

Yogesh P, Dr. Alok Kumar Rohit
Department of Mechanical Engineering
B.Tech Student , School of Engineering & Technology
Jain University, 562112, Bangalore, Karnataka.

Abstract :- This review paper provides the latest researches in the various fields of robotics to make daily routine work more comfortable, convenient, efficient, and economical. This paper deals with different category of robots like climbing robots, eyelid closure robots, facial wearable robots, flying UAV, swarm robots, and fish bio robotics. Eyelid closure robots will be very much helpful for facial paralyzed patients. Robots working with camouflage properties with high resolution of pattern, area of the pattern, and robustness against the failure of an individual is presented in this paper. Fish bio-robotics in the field of biomechanics play an essential role in the field of the hydrodynamics of self-propulsion. Information on different functionality of robots with different parts and components working efficiently is presented here.

Keywords:- Wall Climbing Robots, Flying UAV, Bio Robotics, Swarm Robots.

I. INTRODUCTION

Now a day's robots are very much popular because of their working capability and enhanced form of efficiency. In every working place we have certain kind of robots to save our time and money. In research and development point of view every company shifted towards innovation of more capable and economical working robots with better efficiency. Current scenario robots are working in every field like Medical, Navigation, Automobile industries, Aviation, Marine, Social interaction, Mining, Space & Satellite systems. The era of robots started in the mid of 1954 with a robot called Unimate invented by George Devol. Generally, robotics is the combination of 3 major engineering branch like mechanical, electrical and computer science engineering. Tele manipulators were the origins of the current every kind of robots. In India Hindi speaking humanoid robot named as Rashmi was developed by Ranjit Shrivastava. Its shows that robotic research going on in every part of the world progressively.

II. ADVANCEMENTS IN ROBOTICS

A. Narrow Wall Climbing of Six-Legged Robot

Wheel based robot has limitations in rough terrains. Crawler robot is good over rough terrains but may face instability issues over various other terrains. Legged robots are efficient in locomotion over all terrains irrespective of the roughness. In narrow spaces like pipes/ ducts that are inaccessible to humans, robots are sent for inspection and checking but most of the time it's tough for robots in manipulation i.e. performing the repairing task skillfully. This paper is about a robot named ASTERISK which is designed and developed for basic manipulation tasks. It has 6 limbs with each limb having a mechanism for both locomotion and basic manipulation. This paper is focused on the gait strategies of legged robots' locomotion in narrow spaces particularly for climbing. Also, these gait strategies are less power consuming which is economical [1].

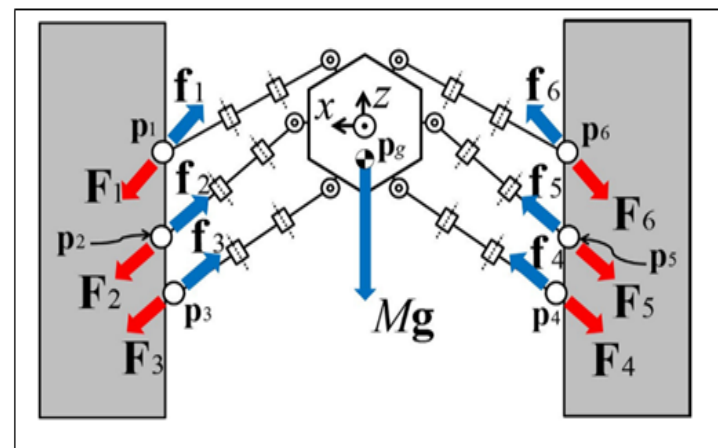


Fig 1:- Climbing Robot Force Distribution

➤ Limb Mechanism Robot ASTERISK

This robot can be used for locomotion or manipulation according to the level of work. The robot's mobility is homogeneous and has omnidirectional manipulation i.e. it receives or transmits signal in all directions. This robot's each limb has 3 rotational joints. So, 6 limbs make the robot have 18 DOF (Degrees of freedom) [2]. The robot weighs about 2.67kg and is of 180mm height at its stable position. Each rotatable joint has DX-117 servo as its main component that includes a servo motor, reduction gear, a control unit, and a communication interface. The best part about their servo is that it produces enough torque to support ASTERISK to stabilize only with three limbs.



Fig 2:- Robot ASTERISK

➤ Proposed Gait Strategies

The team has proposed a "Static model between parallel walls". This model opens up the balancing of ASTERISK between the parallel walls using the pressing force at the tip of the limb. The distance between the parallel walls and also the distance between the body (hexapod structure) and walls is determined by the legs' workspace with experimentation[3]. For the limbs' tip not to lose grip they have used a hemispherical silicon rubber that grips the robot at a height above the ground level. The robot's limb has two phases: a) if the force exerted on the wall by the limb is zero, then it is the swing phase. b) if the force exerted is a bit greater than zero, then the limb is in the support phase.

➤ Gait Strategies to Climb on Parallel Walls

ASTERISK follows two types of strategies to climb parallel walls namely: a) Vertical body climbing gait b) Horizontal body climbing gait. Here the robot's locomotion and motion sequence are that 2 limbs swing free when the other 4 limbs are in the support phase. The two gait strategies differ in their motion sequence of the limbs.

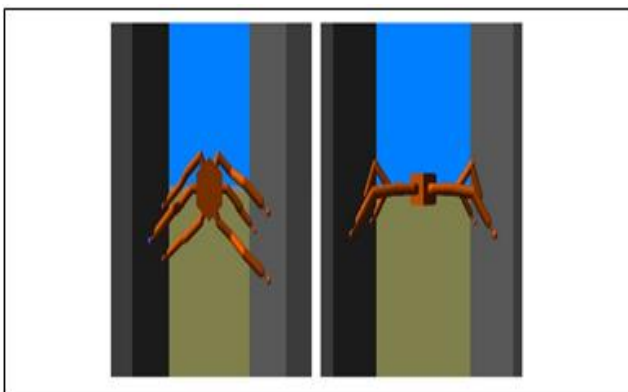


Fig 3:- Vertical & Horizontal body Climbing

➤ A Static Model of Gait Strategies

The gait strategies propose that the swing limbs move symmetrically across the robot's z-axis. They establish equalities of the robot's limb pair that is in support phase to make and understand the stability above ground. The equalities involve the force vector at the tip of each pair of the limb in support and its position vector. Thus they

establish an equilibrium of forces along z-axis and equilibrium of moment of inertia around the z-axis.

➤ Evaluation of Gait Strategies

Here they evaluate their strategies first in simulation and then a real robot.

➤ Simulation

Using 'Open Dynamics Engine (ODE) they developed a dynamic simulator to evaluate their strategies. In that simulator, they structured ASTERISK using basic 3D objects. The rotatable joints' characteristics were taken from the dynamixel servo's specification i.e. compliance and maximum Torque. For vertical body climbing gait, they set the distance between the walls as 60 cm and for horizontal climbing gait it is 70 cm, looking upon to the workspace of two strategies, the horizontal climbing gait has a larger workspace. The two strategies share the simulation parameters which are: a) Gravitational acceleration (m/s^2) – 9.8 b) Coefficient of static friction between limb and wall – 0.85 c) Vertical motion per cycle(m) – 0.06 d) Cycle duration (s) – 6. Simulation outcomes of these two robots were successful but at times the robot fell which made them feel to consider the robust control for the body rotation.

➤ Experiments with Real Robots

With the simulation results being successful the team moved to the real test with ASTERISK. All parameters were the same as a simulator and parallel walls were made of acrylic boards with a robot's limb tip as silicon rubber which is helpful to increase friction. The robot's initial starting position was near the ground and in between the walls. The robot was successful in performing the cycle of corresponding strategies and executed several gait cycles. The torque output required to balance the robot was suitably agreeing with the one from the simulations. In the initial phase of experimentation, one gait cycle took 6s, but after some time, it extended to 12s due to the delays in servo feedback. This delay was because different servo exhibited high torques which caused servo failure. So, the team concluded that the load at each servo should be reduced to improve gait strategy performance.

➤ Power Efficiency Model

For the challenge the team was facing now they had come up with an idea and proposed a power efficiency model. This model aimed at reducing the output torque which is the reason for servo failure. Relating and equating various parameters like current, servo torque, torque constant, voltage, power, and energy. The team came to a viewpoint that required energy is proportional to the total servo torque consumed over the period. Their power efficiency strategy hence minimizes the output power torque [4]. Also, the posture and position of the limbs determine the pressing force (even for small torques). So, they thought of improvising the limb position and posture to provide sufficient force at the tip of the limb within the workspace itself. By this, they minimize the sum of output torques during a cycle. Evaluating this power efficiency model with various parameters like joint angles, length of

each limb link, and no. of support limbs, the team determined the best way for each supporting limb during a cycle. They plotted graphs to get various trajectories. So, the vertical direction of the trajectory is best suited.

➤ *Power Efficiency Evaluation*

After coming up with the model, the team evaluated it in the simulator and then in a real robot. Hence the total output torque is decreased by about 18% compared to the initial one. So, a decrease in output torque means it is also decreasing in power consumption. Thus, the robot is energy efficient.

B. Robot for Movement Assistance on Eyelid Closure

Wearable robot for supporting human movement has gained considerable attention in recent years. The wearable robots have their main purpose in providing physical therapy, enabling semi-automation of therapeutic tasks and to improve movement reproducibility [5]. One of the efficient pioneering works in this field is a robot suit 'HAL' by CYBERDYNE Inc. which supports human gait function based on the wearer's intention using surface myoelectric potentials. A current area of focus in wearable robots is in the articulation of body joints. But the future scope of wearable robots is towards facial movements. This paper is on the application of facial movement in wearable robots.

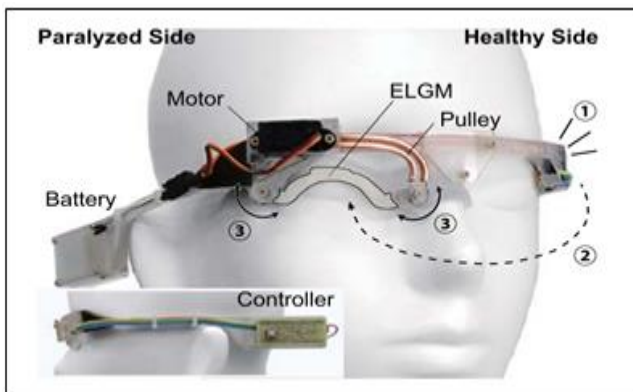


Fig 4:- Eyelid Gating

Out of various types in paralysis, facial paralysis is one which primarily is losing control of the facial muscles on one side of the face. Per year 4 out of 10,000 people are suffering from facial paralysis. Facial paralysis causes severe distractions out of which the inability to close an eyelid leads to various defects in the eye. The health issues caused due to non-closure of the eyelid are a) Exposure of the eye to debris and dryness b) Chronic irritation and pain c) Permanent corneal damage d) Ulceration or infection. The robot here is a non-invasive one that supports eyelid closure with a newly developed mechanism called 'Eyelid Gating Mechanism (ELGM)'.

➤ *Requirements*

We, humans, blink once in 4s on an average and the duration spent in eyelid closure during a blink is 334ms. The process of blinking involves two muscles: a) Orbicularis oculi (sphincter muscle) which are responsible for eyelid closure. b) Levator (striated muscle) which is innervated by the oculomotor nerve and is responsible for eyelid opening. Facial paralysis is a facial nerve disease where patients cannot control the orbicularis oculi and so they cannot close their eyelids [6]. The tarsal plate is a dense connective tissue which supports the eyelid form as a frame and also supports for eyelid movement. The team found the locus of this tarsal plate as a requirement for eyelid movement and manipulation. To develop their idea into a wearable robot they had the following requirements to be met: a) Gentle and safe manipulation b) Lightweight and ease of daily use c) 3D movement along the locus of the tarsal plate. d) Responsive and robust against eyelid movement which is repetitive and quick.

➤ *Eyelid Gating Mechanism (ELGM)*

The team came up with a mechanism that met with their requirements namely the ELGM-eyelid gating mechanism. The various features of this mechanism are a) Simple rotational actuation to 3D-complex motion. b) Rigid actuator-rotational motor c) Responsive and robust movement. d) Soft end effector e) Good affinity f) does not overload or strain on the eye.

➤ *Design Rule of ELGM*

The ELGM is made of a supporting part, two handle parts and a fixed base (with hinges). All these parts are fixed upon an eye-glass type frame. The team, designed the mechanism used 'SolidWorks' and printed it 3D on Object 500 Connex2 3D printer using VeloClear as rigid material and Agilus 30 as soft material [7]. They took 'the anthropometry of Asian eyelids' as a reference for the width between upper and lower eyelids as 7.5mm to 9mm and width between rail an inner corner of the eye as 20mm to 30mm. width the reference they defined 2 parameters which are: a) distance between both hinges=42mm b) inclination of hinges = 400

➤ *Deformation Analysis of the ELGM*

They analyzed the designed parts using 'ANSYS' and defined the ELGM material as hyperelastic material in the simulator. After several positions and tests, they came up with deformation analysis and an exploratory prototype.

➤ *Facial Wearable Robot*

This prototype was put in action and the robot was made up of a lithium-ion battery, controller, sensor, actuator, and the ELGM. This robot detects eyelid movement on the healthy side. Eyelid movement triggers support. Rotational actuation input from a motor is transmitted to the ELGM via a pulley-wire system to manipulate the eyelid on the paralyzed side. The size of the robot is 155x205x25mm and it weighs about 90.1g. This robot specially detects eyelid closure using an IR reflective optical sensor.

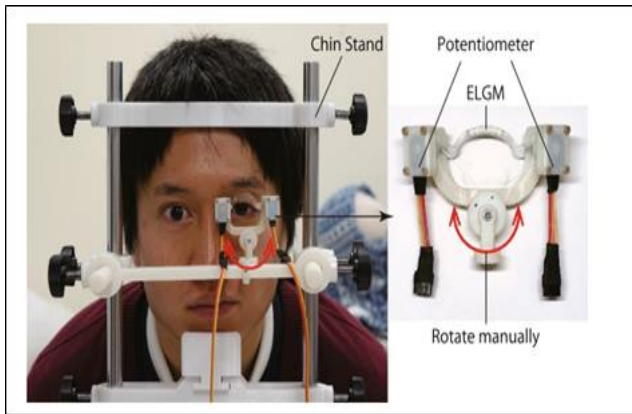


Fig 5:- Facial Wearable Robot

➤ *Eyelid Movement Detection*

This robot works and helps the paralyzed side by tracking the eyelid movement on the healthy side which acts as a trigger for motion support. Eye closure can be detected using various methods out of which the team decided to follow eye wink detection using a reflective optical sensor. The reason for them to follow this method is because eye wink is said to be strong and voluntary eye closure motion. This method is more effective than others because using a reflective optical sensor is contactless and it detects a voluntary motion which is a wearer's intention. This sensor was installed on the healthier side and calibrated accordingly. The graph plotting was done every 10ms with skin displacement signal (converted into threshold frequency). The main advantage of this robot was that the wearer was able to set the threshold by voluntary motion and senses it by a blinking LED and applied vibration. This robot is user-friendly and requires very little time for the wearer to adapt to this.

➤ *Eyeglass-Type Frame*

The data from the scanner will be exported to SolidWorks (CAD) and their process of designing the whole robot (like adding components) is done. This designed robot is 3D printed using two materials one rigid (Velo Clear) and the other one is soft (tango Black Plus) [8]. The soft material is used to set the robot on the head of the wearer. This makes the robot user-friendly because the user requires very little time to put on or remove the robot.

➤ *Evaluation of ELGM*

• *Setting*

As discussed before the facial paralyzed patients can open their eyelids but cannot close. The team welcomed 10 people with complete facial paralysis. Every participant had different facial topologies so the team set a chin stand and a setting where ELGM was early set to the person. The participants were told to relax their facial muscles and blink 5 times with the ELGM set on their paralyzed eye. All the movements were captured by the team using a camera with a frame rate of 60fps. The team then worked on with the calculations from the results obtained. Also, they told the participants to rate the level of stress felt. The team came up with palpebral aperture ratio (PAR) which tells us if the

eyelid is closed completely PAR is 0% and if the eyelid is fully open PAR is 100% [9].

• *Setting*

The team had a plan to check the effectiveness of the robot. For these two people were called one used the eyelid movement detection and another used the eyelid movement support with ELGM. So, here one person blinks his eye and simultaneously the ELGM at another person's eye will blink accordingly. Then one person was blinking with his left eye sensed using the reflective optical sensor and transferred to another person's right eye simultaneously. The team again captured these with a camera with a frame rate of 60fps with which they calculated the PAR.

C. *Formation Flying for Blended-Wing UAV*

Formation flight is the disciplined flight of two or more air vehicles under the command of a flight leader. Current researchers have been working on this domain in various parts of the world. This domain has its source to the large flock of birds flying in v-type formation. Aerodynamicists then developed flights that showed improvements in aerodynamic efficiency than the birds in formation flying. The formation of these flights had two divisions one was tight formation and extended formation [11]. Various researchers in the domain of formation flight have come up with different works in CFD simulation for extended and tight formation and study of their drag reduction in subsonic and transonic flows. Another one used a discrete vortex filament method which included fluid physics with viscosity, Reynolds number and basic parameters of formation flight. Formation flight was initially focused on manned aircraft in less number for military and civilian applications. But in the other case, the formation flight of UAV was focused and case studies about the strategic and tactical advantages of having more number of UAV in formation flight brought in ideas and research on UAV swarms.

Out of many diverse ways of analyzing and simulation process, the team from a CFD viewpoint for capturing wake vortex physics tried for Direct Numerical Simulations (DNS) and Large Eddy Simulations (LES) but they prohibited these due to their immense cost. Finally, they came up with Reynolds Average Navier-Stokes (RANS) which helps them effectively capture the important attributes of these flows. With an option of whether to opt 2D or 3D computations, they preferred 2D because it can be used at an initial phase for a large number of test cases in a short time compared to 3D computations. The team came up with 17 formation types in 2D computations based on which investigations were conducted and results were a benefit to the current world in various fields with good applications.

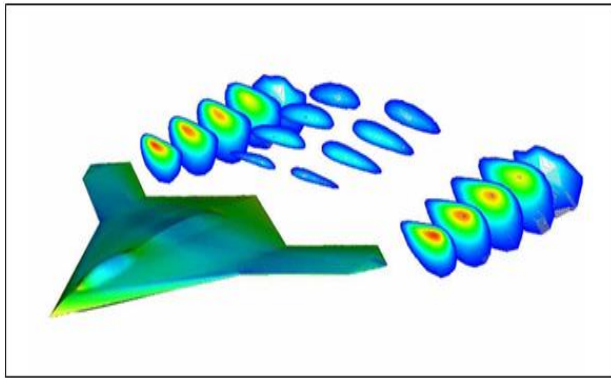


Fig 6:- Flying UAV

➤ Framework Modeling

A physical phenomenon like evolution, decay, a transition to turbulence, boundary layer separation, shock waves, and wake formation was very accurate when using the "Navier-stokes equation" from fluid dynamics. The team to put in a 3D grid for inviscid simulation with 1.5 to 2 million elements took them 1 to 3 days with a modern desktop computer running with 6 CPU's. So they decided to work in 2D for investigating more number of test cases in a short period. Modeling of induced drag effects and wake vortices cannot be computed in 2D but the great advantage is RANS parameters i.e. Reynolds number, viscosity, and compressibility effects can only be applied while computation is done in 2D [12]. More parameters taken for the simulations are like inviscid fluxes, viscous fluxes, free-stream Mach number (M_∞), Boussinesq's approximation, and many more.

➤ Solver Description

The Rusanov Riemann solver and Green Gauss method were taken as the in-house solver for the simulation at transonic speeds. To bring the time to steady-state, the LU-SGS time discretization scheme is employed. The team performed more than 40,000 iterations for obtaining the stabilized drag.

➤ Geometry and Grid Generation

The design and geometry of this UAV is base on UAV "Corax/Raven" of the BAE systems (the team's support organization). The CFD analysis is done using the top view and the wingspan of 10m. The side view was restricted to the formation. The team used grid generation software where unstructured grid with triangular elements and excluding the quadrilateral elements was generated for the far-field. One UAV configuration used upon 29,962 elements in grid generation software.

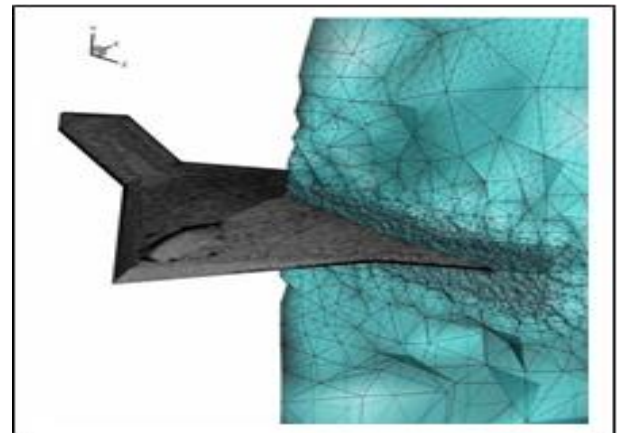


Fig 7:- Grid Model

➤ Simulation Set-Up

The first simulated two and three UAVs to find the stream-wise optimal distance which they used for all the test cases. Here the main parameters they consider are drag whose reduction is computed as the average drag from the formation which is the improvements in aerodynamic efficiency that the team focuses on.

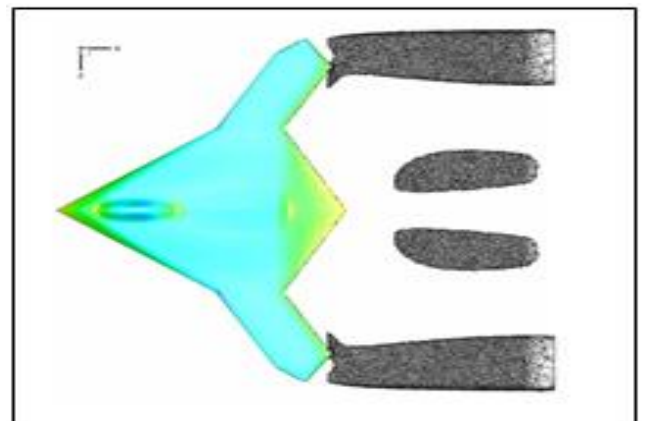


Fig 8:- Free-Stream Conditions

➤ Proximity Analysis

Since the computation is done purely in 2D. So, the coordinate axis will be x and y axes. Thus two proximity analyses were performed namely y-proximity analysis and x-proximity analysis. The y-proximity analysis goes like this, the distance between the wingtip to the tip distance zero was taken into account and this value may be negative as the tip of the follower UAV is positioned inside the leader's wake. From the literature study, the team understood that the smaller the tip to tip distance the greater drag reduction [13]. On the other side for x-proximity analysis, the stream-wise distance of aircraft was taken concerning the wingspan distance between two UAVs. They concluded the x-proximity analysis that greater drag reduction was seen with greater wingspan distance and by analysis, it was 3 wingspan distance.

➤ *Simulation Matrix*

They simulated and tested 18 test cases of formations as 9-echelon, 4 v-types, 2 diamond, and 2 half diamond.

D. Distributed Camouflage for Swarm Robotics and Smart Materials

Animals at times use camouflage to be safe from predators. Camouflage in engineering has its great scope in military and defense domains. Here sensing and control are highly relying factor of camouflage of animals other than the visual. In nature, the animals' camouflage exactly matches the background which is a tough complicated work to do with robots. So, the team is focused to at least fool the predator by the basic pattern forming camouflage with the background. The team puts on various factors for camouflage generation like a) resolution of the pattern b)

area of the pattern c) robustness against the failure of individual units. Here a swarm of droplet robots has been used, these robots sense and response to color by emitting and have fast communication with the nearby swarm.

The important factor required here is local sensing of color, computation and also process the signals with sensors. The group uses three-step of the process in their algorithm they are: a) estimate color and gradient histogram b) process the parameter for pattern c) finally reaction-diffusion process which puts up the pattern on the swarm. A two-tone pattern approach for color identification is used here. High resolution of picture/background is converted to low resolution by a discrete convolution operation so that pattern making can be easy for the swarm.

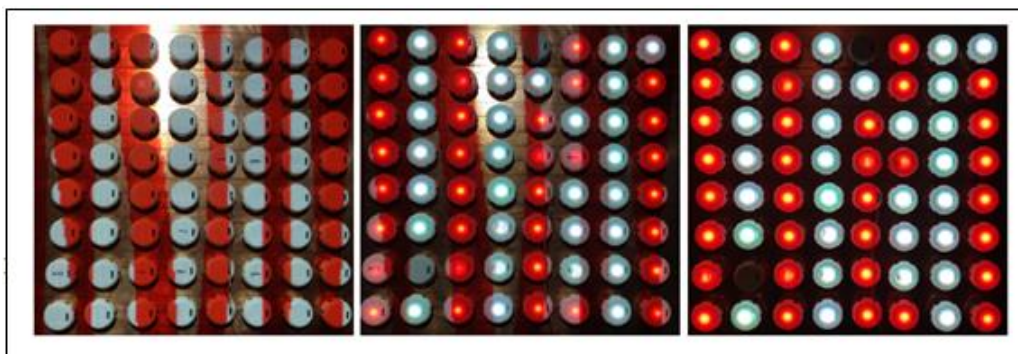


Fig 9:- Pattern Display

➤ *Distributed Camouflage Algorithm*

The robot uses a sensor that detects the color projected on it and then shares it with nearby robots. Every robot computes a pattern based on the received information. The probability function is used here by the robots to calculate the local probability. After all, a global pattern is accepted by the swarm and shows the pattern using a reaction-diffusion process.

➤ *Pattern Descriptor*

They use a concept that is widely used in computer vision and edge detection in kernels by which the robot applies discrete approximation in both directions for the information obtained in horizontal and vertical. Here the robot is represented as a pixel where the swarm is the whole pattern (image) [14]. The two-tone approach includes the two pattern descriptors which are the pixel color value after every two convolutions. As mentioned the pattern descriptors are second-ordered derivatives used to calculate probable local patterns.

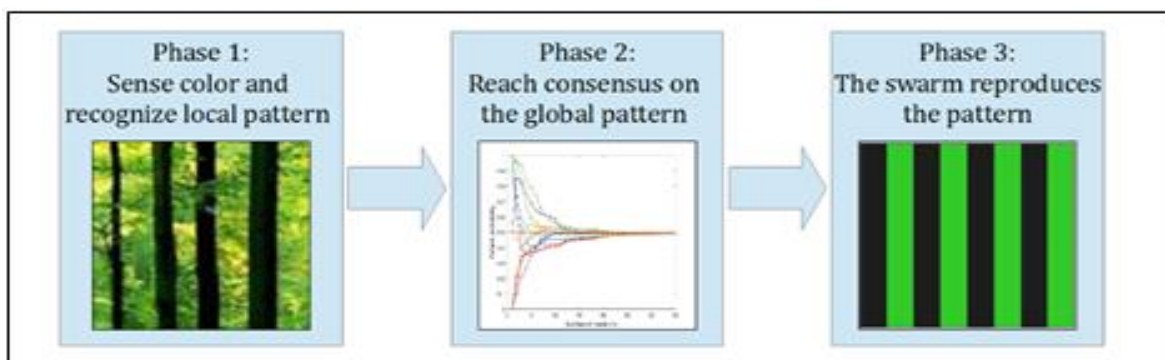


Fig 10:- Camouflage Algorithm

➤ *Distributed Average Consensus Scheme*

Here the weighted-average local pattern is calculated using Metropolis weights. The robot after all computations accepts one pattern as a global pattern that is largest among

other average local patterns shared between the swarm robots. This usage of Metropolis weights is simple and best for distributed algorithms.

➤ Pattern Generator

The robot swarm after achieving a global pattern next has its move to display the pattern. So, the team uses the activator-inhibitor model with which generation and communication of patterns between the robots are much simpler. In this model, the robot can be either on or off and forms a morphogenetic field comprising the activator and inhibitor morph gens. The activator morph gen is kept inside the inhibitor and activator responds to nearby 'on' robots whereas the inhibitor responds to nearby 'off' robots. The robot swarm undergoes a series of on, off switch states till they form a stable pattern. The pattern is generated as horizontal, vertical first and then the final as the mottled pattern.

➤ Simulated Results

For the simulated test, the team chose 3 grayscale pictures of 128 X 128 pixels. They used 64 robots with the swarm assembled in 8 X 8 formations. The captured pictures were less resolution with 8 X 8 pixels so, they fed the input image as a 16 X 16-pixel blocks. The image was blurred so it was easy for the swarm to understand the pattern and to choose a color. Further for pattern, the blurred image was converted to binary colors i.e. black and white. Here W1 (activator field value) and W2 (inhibitor field value) was set as parameters for pattern generation. For the best results, the values obtained were $W1 = 1$ and $W2 = -0.75$. As they started estimating errors, they saw that errors rose sharply but the pattern displayed by the swarm was still good. The conclusion they obtained from the simulation is that "the resulting pattern fits well even with large errors".

➤ Hardware Implementations

The team had their next move towards creating the hardware of the robot swarm. They created a swarm of droplets which is an open-source platform. These droplet robots are cylindrical in structure and have various components like alternating power strips for +5V and GND, Atmel x Mega128A3u microcontroller, 6 infrared emitters, receivers, sensors, RGB LED. Each of these robots has a unique 16-bit ID. In this implementation the team came up with 4 phases they are: a) Phase0-neighbour ID identification b) Phase1-color sensing and recognition c) Phase2-pattern consensus d) pattern formation. Each phase is allotted certain frames according to their requirements.

E. Fish Bio-Robotics: Kinematics and Hydrodynamics of Self-Propulsion

Biomechanics in aquatic animals has been a great area of research from far long days. The variants in the usage of muscles for locomotion are the great areas of focus for research and biologists. The initial phase in this aquatic propulsion was started around 1912 using basic mechanical models. Then this field of aquatic propulsion developed various new and groundbreaking researches and works. Currently, the work is to perfectly mimic the fish and its motion in various natural conditions [16]. This paper discusses various investigations on fish locomotion and how various fins are functioning structurally to support the motion. Here the team uses a self-propelled robotic device with which they find out the propulsion of 3 categories of fins namely: Pectoral fins, dorsal fins, and caudal fins.

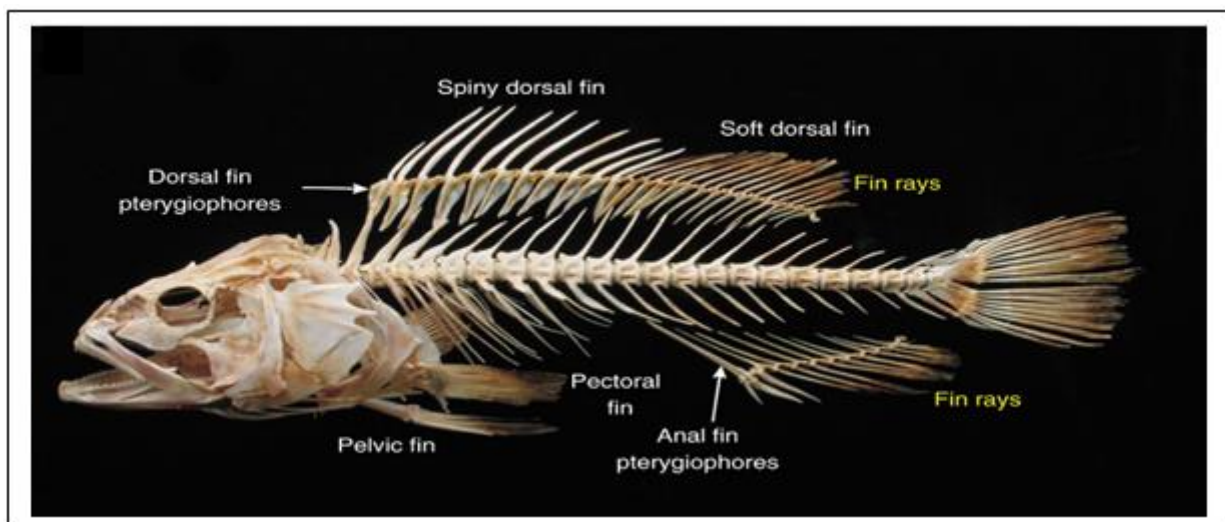


Fig 11:- Fish Fins

➤ Fish Locomotion: Function of Paired and Median Fins in Vivo

The motion in a fish is due to its three structural areas i.e. body, paired and median fins. The fins generate forces and also help in controlling the movement and body's position in various circumstances. Each fish has its skeletal structure, musculature but its fins are one which supports the surface movement. Here the paired fin structure is

pectoral fins and midline structures are dorsal, anal and caudal fins. The team says, theoretically interactions between the pectoral and median fins are possible but no practical experimentations have ever been done in the domain of aquatic propulsion in fishes. So, the team for practical experimentation tested the pectoral and median fins separately.

➤ Paired Fin Propulsion: Pectoral Fins

For this study, the team used a high-resolution megapixel camera which is used to analyze quantitatively the fin bending and propulsion from individual fin rays. Here the team has chosen the bluegill sunfish for their study. The pectoral fin movement has two-phases of movement they are: a) twisting-chard wise and spanwise

bending b) cupped shaped [17]. These phases result in an expansion of the fin area and curvature of the fin during bending and twisting. Throughout the fin beat cycle, the velocity of water in downstream is more when compared to free-stream. This gives them an idea that thrust is produced during the cycle and two peaks are obtained due to outstroke and in-stroke of fin movement.

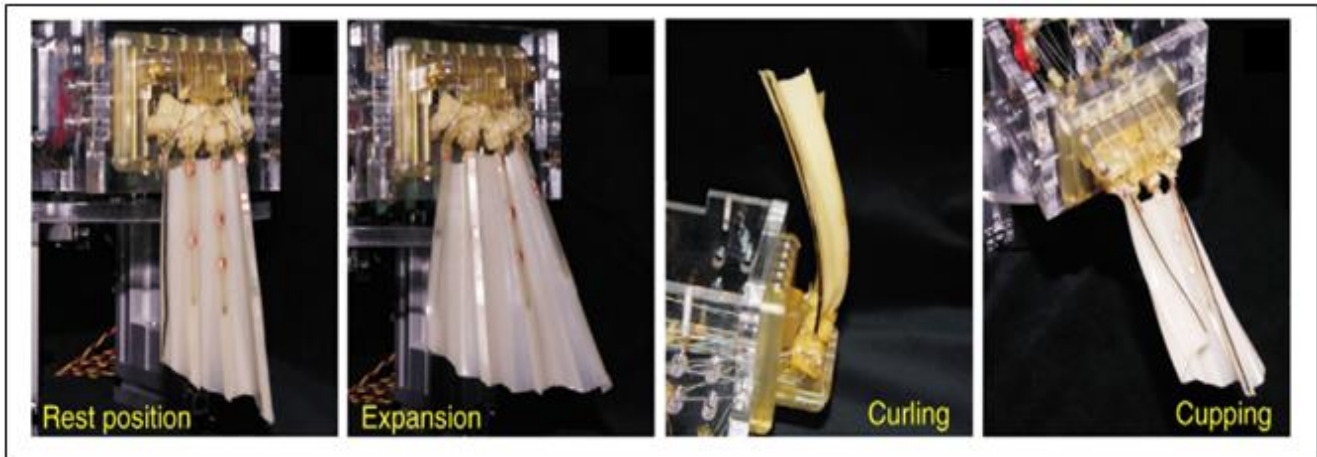


Fig 12:- Fish Movement Mechanism

➤ Median Fin Propulsion: The Body, Dorsal, and Anal Fins

The dynamics of locomotion in fishes are mainly due to the dorsal and caudal fins collectively called the median fins. In bluegill sunfish, lateral movement is possible through the soft dorsal and anal fins but this movement isn't supported or made possible with the fish's spiny-finned dorsal. The major fin contributors are soft dorsal and anal fin because, they are always active during various movements and especially during slow swimming, the wake vortex, the force created by them is as equal to that of the tail. The wake vortex created here by the fish enhances the thrust produced by the tail when it is at the proper position.

➤ Fish Locomotion: Studied with Robotic Models

Robotic models of fishes are used in 3 ways of approach they are: a) One is to simultaneous study the force generated in a controlled pattern in still water or flow tank b) Another way is to tow the robot in water and find out the thrust, force, torque generated using sensors in areas of flapping foil robots' propulsion study c) The modern way or the self-propulsion technique is the equalization of thrust and drag force of the robot in both upstream and downstream motions [18]. The team used various parameters like flow speed, position in a flow tank to evaluate the thrust, lift forces and side forces during self-propulsion. The only problem they faced in the practical test was the power and sensor cable has its force on the robot. This problem was combated by the robot's position in the flow tank.

➤ A Robotic Fish Pectoral Fish

The team prepared a bio-robotic fin made up of nylon tendons that were motor controlled and the fin had five bilaminar fin rays with the modulus of elasticity of

approximately 0.10 MPa. The robot model had multiple-segmented flexible merely like the fin of a real fish. The reorientation of the fin was set as $\pm 60^\circ$ pitch and 180° yaw movements. This model used the air bearing, force transducer to measure the thrust generated by the fin carriage. The robot's fin movement was the combination of all three phases of locomotion in a real phase i.e. curl, expansion and cupping. Sinusoidal waves were given as signals for the robot's movements in curl and expansion. But square waves were given for the robot's cup-shaped movement [19]. As we saw the two thrust peaks generated by the fish in outstroke and in-stroke the robotic fins also result in the same when in the cup and sweep motion. Thus for thrust generation, the cup phase of locomotion is very much necessary whereas sweep has only very little net thrust to contribute. Even though the results were satisfactory the robotic model gave a negative thrust at mid-stroke for a very short period.

➤ A Flapping Foil Robot

The median fins are considered as dual flapping foils in series. As discussed previously, the dorsal and anal fins are upstream creating a wake vortex which is faced by the caudal fins as downstream. This flapping foil robot is used to execute a variety of new patterns and create different wake vortexes. It is useful in finding out the flexibility of the robot along with the interactions between the foils of the robot. This robot has independent self-propulsion due to their carriages which are attached to an air bearing system. The area of bio-propulsion is still not very accurate with the current findings thus this flapping foil also helps us to estimate biometric foil's flexibility. Flexible hydrofoils are currently being used in aquatic systems to measure thrust for fin and body propulsion.

III. CONCLUSION

This review paper provide specific and collective informations of robots working in various fields. Paper will be helpful for beigneers to explore in the field of medical, marine, aviation and automobile industries. Now a days robots helping for business owners and creating more competitive environnment for others. Robots can reduce the delivery time and can work in more efficient manner. So robots in future will become the Milestone for entire world.

REFERENCES

- [1]. Ohara, K., Toda, T., Kamiyama, K., Kojima, M., Horade, M., Mae, Y., & Arai, T. (2018). Energy-efficient narrow wall climbing of six-legged robot. *ROBOMECH Journal*, 5(1). <https://doi.org/10.1186/s40648-018-0121-y>.
- [2]. Takubo T, Arai T, Inoue K, Ochi H, Takeshi K, Tsurutani T, Hayashibara Y, Koyanagi E (2006) Integrated limb mechanism robot ASERISK. *J Robot Mechatron* 18(2):203–214.
- [3]. Grieco JC, Prieto M, Armada M, de Santos PG (1998) A six-legged climb- ing robot for high payloads. In: Proceedings of the 1998 IEEE international conference on control applications, pp 446–450.
- [4]. Zarrouk D, Fearing RS (2013) Cost of locomotion of a dynamic hexapedal robot. In: Proceedings of the 2013 IEEE international conference on robotics and automation, pp 2533–2538.
- [5]. Kozaki, Y., Matsushiro, N., & Suzuki, K. (2018). A wearable soft robot for movement assistance on eyelid closure. *ROBOMECH Journal*, 5(1), 1–9. <https://doi.org/10.1186/s40648-018-0126-6>.
- [6]. Kozaki Y, Suzuki K (2017) A facial wearable robot with eyelid gating mechanism for supporting eye blink. In: Annual international conference on intelligent robots and systems, pp 1812–1817.
- [7]. Leigh RJ, David SZ (2015) The neurology of eye movements. Oxford University Press, Oxford.
- [8]. Robin S, Everett C, Anne L, Zofia L (1990) The eye wink control interface: using the computer to provide the severely disabled with increased flex- ibility and comfort. In: Proceedings of third annual IEEE symposium on computer-based medical systems. IEEE, New York, pp 105–116.
- [9]. Uav, A. B. (2017). *Parametric Study on Efficient Formation Flying For*. 1657–1664.
- [10]. Antoniadis, P. Tsoutsanis, and Drikakis.D., “High-order schemes on mixed-element unstructured grids for aerodynamic flows,” in 42nd AIAA Fluid Dynamics Conference and Exhibit, AIAA, Ed., no. AIAA 2012- 2833, New Orleans, Louisiana, June 2007.
- [11]. S. A. Ning, T. C. Flanzer, and I. M. Kroo, “Aerodynamic performance of extended formation flight,” *Journal of Aircraft*, vol. 48, no. 3, pp. 855–865, 2011.
- [12]. T. Gerz and T. Ehret, “Wingtip vortices and exhaust jets during the jet regime of aircraft wakes,” *Aerospace Science and Technology*, vol. 1, no. 7, pp. 463–474, 1997.
- [13]. Li, Y., Klingner, J., & Correll, N. (2018). Distributed camouflage for swarm robotics and smart materials. *Autonomous Robots*, 42(8), 1635–1650. <https://doi.org/10.1007/s10514-018-9717-6>.
- [14]. Fekete, S.P., Fey, D., Komann, M., Kröller, A., Reichenbach, M., Schmidt, C.: Distributed vision with smart pixels. In: Proceedings of the twenty-fifth annual symposium on Computa- tional geometry, pp. 257–266. ACM (2009).
- [15]. Morin, S.A., Shepherd, R.F., Kwok, S.W., Stokes, A.A., Nemiroski, A., Whitesides, G.M.: Camouflage and display for soft machines. *Science* 337(6096), 828–832 (2012).
- [16]. Yu, C., Li, Y., Zhang, X., Huang, X., Malyarchuk, V., Wang, S., Shi, Y., Gao, L., Su, Y., Zhang, Y., et al.: Adaptive optoelectronic camouflage systems with designs inspired by cephalopod skins. *Proceedings of the National Academy of Sciences* 111(36), 12,998–13,003 (2014).
- [17]. Lauder, G. V., Anderson, E. J., Tangorra, J., & Madden, P. G. A. (2007). Fish biorobotics: kinematics and hydrodynamics of self-propulsion. *Journal of Experimental Biology*, 210(16), 2767–2780. <https://doi.org/10.1242/jeb.000265>.
- [18]. Lauder, G. V. and Drucker, E. G. (2004). Morphology and experimental hydrodynamics of fish fin control surfaces. *IEEE J. Oceanic Eng.* 29, 556-571.
- [19]. Anderson, J. M. and Chhabra, N. (2002). Maneuvering and stability performance of a robotic tuna. *Integr. Comp. Biol.* 42, 118-126.